

Fine Structure Constant, Electron Anomalous Magnetic Moment, and Quantum Electrodynamics

Toichiro Kinoshita

Laboratory for Elementary-Particle Physics, Cornell University

based on the work carried out in collaboration with
M. Nio, T. Aoyama, M. Hayakawa, N. Watanabe, K. Asano.

presented at Nishina Hall, RIKEN
November 17, 2010

- The fine structure constant

$$\alpha = \frac{e^2}{2\epsilon_0 hc}$$

is a dimensionless fundamental constant of physics:

e = electric charge of electron,

ϵ_0 = dielectric constant of vacuum,

h = Planck constant,

c = velocity of light in vacuum.

- Since α is basically measure of magnitude of e , it can be measured by any physical system involving electron directly or indirectly.

- Some high precision measurements of α :

Mohr, Taylor, Newell, RMP 80, 633 (2008)

$$\alpha^{-1}(\text{ac Josephson}) = 137.035\,987\,5\,(43) \quad [31\text{ ppb}]$$

$$\alpha^{-1}(\text{quantum Hall}) = 137.036\,003\,0\,(25) \quad [18\text{ ppb}]$$

$$\alpha^{-1}(\text{neutron wavelength}) = 137.036\,007\,7\,(28) \quad [21\text{ ppb}]$$

$$\alpha^{-1}(\text{atom interferometry}) = 137.036\,000\,0\,(11) \quad [7.7\text{ ppb}]$$

$$\alpha^{-1}(\text{optical lattice}) = 137.035\,998\,83\,(91) \quad [6.7\text{ ppb}]$$

- However, by far the most accurate α comes from the measurement of **electron anomalous magnetic moment a_e** and the theoretical calculation in quantum electrodynamics (QED) and Standard Model (SM):

$$\alpha^{-1}(a_e) = 137.035\,999\,085\,(12)(37)(33) \quad [0.37 \text{ ppb}]$$

where 12,37,33 are the uncertainties of 8th-order term, estimated 10th-order term, and measurement of a_e .

$$(\alpha^{-1} - 137.036) \times 10^7$$

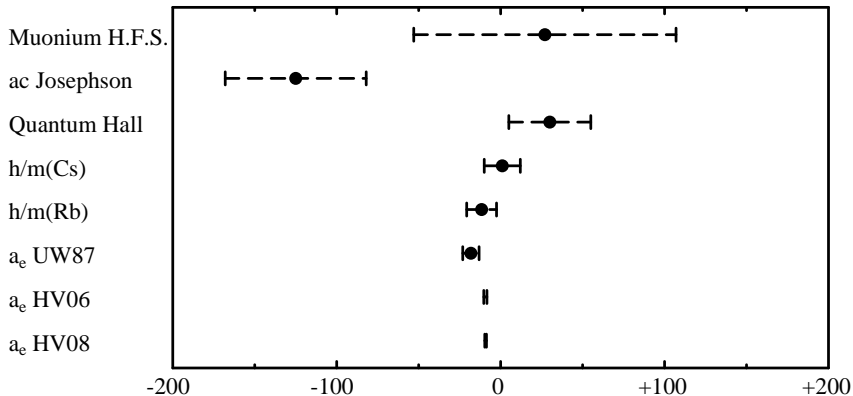


Figure: Comparison of various α^{-1} of high precision.

$$(\alpha^{-1} - 137.036) \times 10^7$$

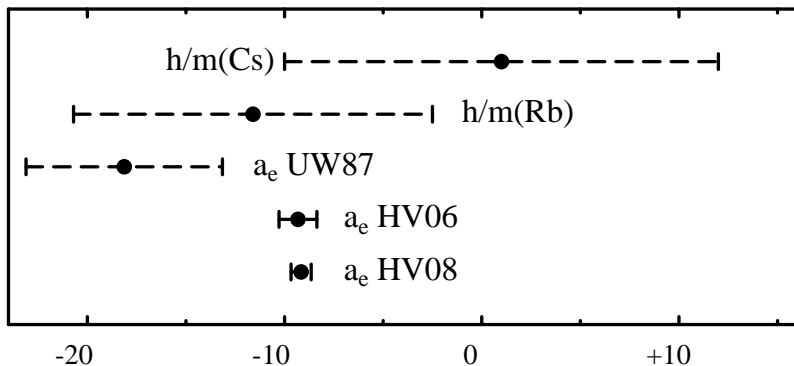


Figure: Magnification of the lower half of the last figure by factor 10.

- $\alpha(a_e[\text{HV08}])$ is 18 times more accurate than $\alpha(\text{Rb})$.

Brief review of QED

- I will discuss how such precise α is obtained from a_e , and possible implication on quantum mechanics (including QED and SM).
- Of course **quantum mechanics** is the basis of our understanding of material world and the foundation of many modern technologies.

Heisenberg, Z. Physik 33, 879 (1925)

Schrödinger, Ann. der Phys. 81, 109 (1926)

- However, it was known from the beginning that it is applicable only to slowly moving particle, **slow compared with the velocity of light c** .
- One way to remove this restriction was found by Dirac who discovered an equation, **Dirac equation**, which **works at any velocity**.

Dirac, Proc. Roy. Soc. (London) A117, 610 (1928)

- Among many successes of Dirac equation is the prediction that **gyromagnetic ratio g of electron** is equal to 2, which agreed with measurement.
- However, Dirac eq. had puzzling feature that it appeared to predict presence of **negative energy states**.
- It turned out that these states can be interpreted as **positive energy states of positron** (which has same mass but opposite charge to electron).
- This interpretation was justified experimentally by the discovery of positron in cosmic ray experiment.

Anderson, Phys. Rev. 41, 405 (1932).

- Formally this is equivalent to treating electron and positron as operators of quantized Dirac field.

- By 1929 relativistic quantum field theory (QED), which describes the interaction of **electron field** and electromagnetic field, was formulated.

Heisenberg, Pauli, Z. Physik, 56, 1 (1929)

Dirac, Proc. Roy. Soc. (London) A136, 453 (1932)

- Calculation in **2nd order perturbation** of QED for processes such as Compton scattering (**Klein-Nishina formula**), Bremsstrahlung, and atomic energy levels, agreed with experiments within few percents.
- However, when one tried to improve theory by including **higher order effects**, one ran into strange situation that result becomes **infinitely large**.
- QED was thus regarded as seriously sick for many years.
- (In 1939 Kramers was telling people that the divergence problem might be solved by "renormalization". But he had no idea how to work it out.)

- The key to solution was provided in 1947 by two experiments which showed that predictions of Dirac eq. require tiny but **non-vanishing** corrections, thanks to much improved measurement precision due to advances in microwave technology.
- One is **Lamb shift** of hydrogen atom:
 $2S_{1/2}$ level is about 1050 MHz higher than $2P_{1/2}$ level, whereas Dirac eq. predicts that they are at the same level (i.e., degenerate).
 Lamb, Retherford, Phys. Rev. 72, 241 (1947)
- The other is **Zeeman splitting of Ga atom** which showed that g -factor of the electron is about 0.1 % larger than the prediction of Dirac eq., i.e., electron has **anomalous magnetic moment**:

$$a_e \equiv (g - 2)/2 = 0.001\ 15\ (4).$$

Kusch, Foley, PR 72, 1256 (1947)

- These experiments forced people to realize that, mass and charge parameters of QED must be reinterpreted as **observed** mass and charge **minus their radiative corrections**.
- When QED is thus **renormalized**, these divergences disappear from calculated physical processes.
- Bethe applied this idea **within nonrelativistic framework** and obtained the Lamb shift in rough agreement with measurement.

Bethe, Phys. Rev. 72, 339 (1947).

- For unambiguous treatment of renormalization, however, it is necessary to have relativistic formulation.
- Note: **Relation of energy and mass is not fixed without relativity**.

- Such relativistic formulation was being developed by Tomonaga and Schwinger, unknown to each other.

Tomonaga, RIKEN-IHO 22, 545 (1943) in Japanese; Prog. Theor. Phys. 1, 27 (1946)

Koba, Tomonaga, Prog. Theor. Phys. 2, 218 (1947)

Schwinger, Phys. Rev. 73, 416 (1948); 74, 1439 (1948); 75, 651 (1949); 76, 790 (1949)

- Schwinger applied it to a_e and obtained

$$a_e = \frac{\alpha}{2\pi} = 0.001\,161\,300\,94\dots$$

in excellent agreement with the measurement.

Schwinger, PR 73, 416L (1948); PR 75, 898 (1949)

- Together with Bethe's work on the Lamb shift, this provided firm experimental support for **renormalized QED**.

- Over 60 years since then, precision of $g - 2$ measurement has been improved by **eight orders of magnitude** (**spin precession, Penning trap**).
- Theory has also been improved by similar order of magnitude.
- Latest innovations and improvements of the Penning trap method by Gabrielse's group at Harvard led to the precision of 0.24 parts per billion:

$$a_e(\text{exp}) = 1\,159\,652\,180.73 (0.28) \times 10^{-12} \quad [0.24 \text{ ppb}]$$

Hanneke, Fogwell, Gabrielse, PRL 100, 120801 (2008)

- Their cylindrical Penning trap is shown next.

Cylindrical Penning Trap

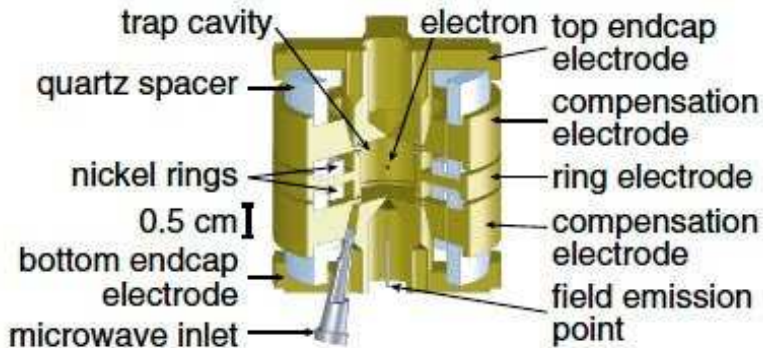


Figure: Cylindrical Penning Trap of Harvard experiment

At Gabrielse's apartment near CERN

Remiddi

Kinoshita

Gabrielse



Basking in the reflected glow of theorists

Feynman-Dyson method

- Simple theoretical structure and availability of precise measurement makes a_e particularly suitable for high precision test of validity of QED.
- However, computational methods of Tomonaga and Schwinger were too cumbersome to handle theory to comparable precision.
- It is **diagrammatic method and use of Feynman propagator** invented by Feynman and elaborated by Dyson that simplifies the calculation enormously and enables us to evaluate $g - 2$ systematically to high orders.

Feynman, Phys. Rev. 74, 1430, (1948); 76, 769 (1949)

Dyson, Phys. Rev. 75, 486, 1736 (1949)



(a) Feynman explaining parton theory, 1962



(b) Freeman Dyson

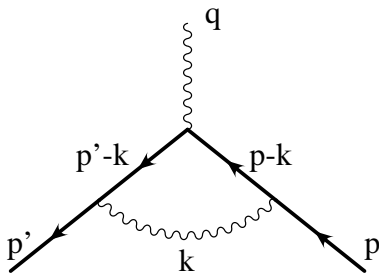


Figure: Feynman diagram: Radiative correction to the scattering of electron from momentum p to momentum p' by the potential (represented by q).

- Feynman-Dyson rule gives:

$$\lim_{\epsilon \rightarrow +0} \int d^4k \bar{u}(p') \gamma^\nu \frac{i}{\not{p}' - \not{k} - m + i\epsilon} \gamma^\mu \frac{i}{\not{p} - \not{k} - m + i\epsilon} \gamma_\nu u(p) \frac{-i}{k^2 + i\epsilon}$$

- Schwinger's formula will be ~ 8 times longer.
- Tomonaga's formula will be even longer.

Following Dyson we can write a_e as

$a_e = a_e(\text{QED}) + a_e(\text{hadron}) + a_e(\text{electroweak})$, where

$$a_e(\text{QED}) = A_1 + A_2(m_e/m_\mu) + A_2(m_e/m_\tau) + A_3(m_e/m_\mu, m_e/m_\tau)$$

$$A_i = A_i^{(2)} \left(\frac{\alpha}{\pi}\right) + A_i^{(4)} \left(\frac{\alpha}{\pi}\right)^2 + A_i^{(6)} \left(\frac{\alpha}{\pi}\right)^3 + \dots, i = 1, 2, 3$$

- First four A_1 terms are known analytically or by numerical integration

$A_1^{(2)} = 0.5$	1 Feynman diagram (analytic)
$A_1^{(4)} = -0.328\ 478\ 965 \dots$	7 Feynman diagrams (analytic)
$A_1^{(6)} = 1.181\ 241\ 456 \dots$	72 Feynman diagrams (analytic, numerical)

Laporta, Remiddi, PLB 379, 283 (1996)

Kinoshita, PRL 75, 4728 (1995)

$A_1^{(8)} = -1.914\ 4\ (35)$	891 Feynman diagrams (numerical)
-------------------------------	----------------------------------

Kinoshita, Nio, PRD 73, 013003 (2006)

Aoyama, Hayakawa, Kinoshita, Nio, PRD 77, 053012 (2008)

- A_2 term is small but not negligible: $\sim 2.72 \times 10^{-12}$.
- A_3 term is completely negligible at present: ($\sim 2.4 \times 10^{-21}$).
- Hadronic and electroweak contributions (in SM) are also known
 - a) $a_e(\text{hadron}) = 1.689 (20) \times 10^{-12}$

Jegerlehner, priv. com. 1996
Krause, PLB 390, 392 (1997)
Nyfeller, arXiv:0901.1172 [hep-ph]

b) $a_e(\text{EW}) = 0.030 \times 10^{-12}$

Czarnecki *et al.*, PRL 76, 3267 (1996)

- If one assumes $|A_1^{(10)}| < 4.6$

Mohr, Taylor, Newell, RMP 80, 633 (2008)

for the unknown 10th-order term, one obtains

$$a_e(\text{Rb}) = 1\,159\,652\,182.79 (0.11)(0.37)(7.72) \times 10^{-12},$$

$$a_e(\text{exp}) - a_e(\text{Rb}) = -2.06 (7.72) \times 10^{-12}.$$

where

$$\alpha^{-1}(\text{Rb}) = 137.035\,998\,84 (91). \quad [6.7 \text{ ppb}],$$

is the value obtained by an optical lattice method.

P. Cladé et al., PRA 74, 052109 (2006)

- Uncertainty 0.11 of $A_1^{(8)}$ and **guestimated error 0.37** of $A_1^{(10)}$ are much smaller than 7.72 of the best measured α available.
- Thus unknown $A_1^{(10)}$ does not appear to be a serious problem.

- To put it somewhat differently, non-QED α , even the best one, is too crude to test QED to the precision achieved by theory and measurement of a_e .
- Thus it makes more sense to test QED by an alternative approach:

*Get α from theory and measurement of a_e
and compare it with other α 's.*

- This yields

$$\alpha^{-1}(a_e) = 137.035\,999\,085\,(12)(37)(33) \quad [0.37 \text{ ppb}],$$

where 12, 37, 33 are uncertainties of 8th-order, 10th-order, and $a_e(\text{exp})$.

- Now the unknown $A_1^{(10)}$ becomes the largest source of uncertainty.

Work on the tenth-order term

- Harvard group is working to reduce measurement error.
- Further progress of theory is not possible unless $A_1^{(10)}$ is actually calculated.
- Thus we began working on the 10th-order term more than 7 years ago.
 - 12672 Feynman diagrams contribute to $A_1^{(10)}$.
 - 9080 Feynman diagrams contributing to $A_2^{(10)}$.
- Clearly this is a gigantic project, requiring systematic and highly automated approach.
 - First step: Classify them into gauge-invariant sets.
 - There are 32 gauge-invariant sets within 6 supersets.

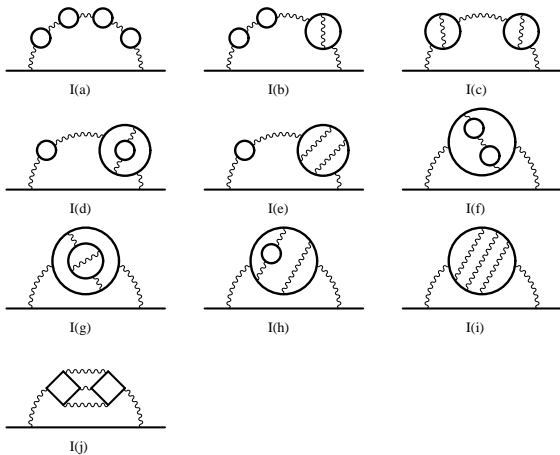


Figure: Diagrams of Superset I.

Set I consists of 10 subsets, all built from a second-order vertex. Solid lines represent electron propagating in magnetic field. Wavy lines represent photons. 208 diagrams contribute to $A_1^{(10)}$. 498 contribute to $A_2^{(10)}(m_e/m_\mu)$.

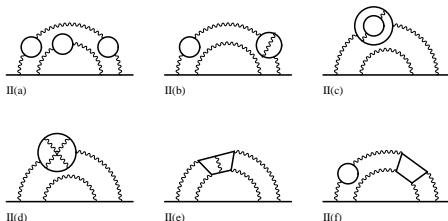


Figure: Diagrams of Superset II.

Set II is built from fourth-order proper vertices. 600 diagrams contribute to $A_1^{(10)}$. 1176 diagrams contribute to $A_2^{(10)}(m_e/m_\mu)$.

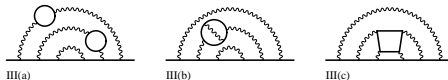


Figure: Diagrams of Superset III.

Set III is built from sixth-order proper vertices. 1140 diagrams contribute to $A_1^{(10)}$. 1740 diagrams contribute to $A_2^{(10)}(m_e/m_\mu)$.

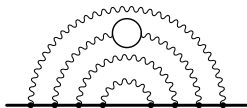


Figure: Diagrams of Superset IV.

Set IV is built from eighth-order proper vertices. 2072 diagrams contribute to both $A_1^{(10)}$ and $A_2^{(10)}(m_e/m_\mu)$.

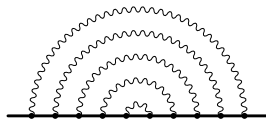


Figure: Diagrams of Superset V.

Set V consists of 10th-order proper vertices with no closed lepton loop. 6354 diagrams contribute to $A_1^{(10)}$. No contribution to $A_2^{(10)}(m_e/m_\mu)$.

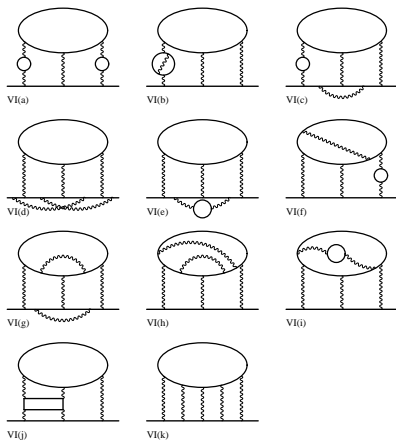


Figure: Diagrams of Superset VI.

This set has 11 subsets, all containing *light-by-light-scattering* subdiagrams.
 2298 diagrams contribute to $A_1^{(10)}$. 3594 contribute to $A_2^{(10)}(m_e/m_{\mu})$.

Tenth-Order Diagrams with Closed Lepton Loops

- Actually, sets I(a), I(b), I(c), II(a), II(b) are fairly simple and even analytical results are known for some of them.

S. Laporta, PLB 328, 522 (1994)

- Analytic integration of other diagrams is far more difficult.
(Recall: Even 8th-order is not yet done.)
- Numerical approach is the only viable option at present.
- This is relatively easy for g-i sets containing only v-p loops.
- We have only to modify known lower-order integrals slightly.

- Diagrams containing **light-light-scattering subdiagram** are much harder to evaluate.
- But we managed to integrate some of them by 2006.
Kinoshita,Nio, Phys. Rev. D 73, 013003 (2006)
- Now we have evaluated all other sets with the help of automatic code generators ***gencodevpN*** and ***gencodeLLN***.
Aoyama,Hayakawa,Kinoshita,Nio, Phys. Rev. D 78, 113006 (2008)
Aoyama,Hayakawa,Kinoshita,Nio,Watanabe, Phys. Rev. D 78, 053005 (2008)
Aoyama,Asano,Hayakawa,Kinoshita,Nio,Watanabe, Phys. Rev. D 81, 053009 (2010)
- Tables on next pages summarize the current status, including those published already.

Table: Numerical values of diagrams of Set I. Preliminary results are indicated by **red**

Set	$A_1^{(10)}$	$A_2^{(10)}(m_e/m_\mu)$	$A_2^{(10)}(m_\mu/m_e)$	$A_2^{(10)}(m_\mu/m_\tau)$	$A_3^{(10)}(m_\mu/m_e, m_\mu/m_\tau)$
$I(a)$	0.000 470 94 (6)	0.000 000 28 (0)	22.567 05 (25)	0.000 038 (1)	0.015 200 (7)
$I(b)$	0.007 010 8 (7)	0.000 001 88 (0)	30.667 54 (33)	0.000 271 (1)	0.020 176 (8)
$I(c)$	0.023 468 (2)	0.000 002 67 (0)	5.141 38 (15)	0.003 936 (1)	0.002 331 (2)
$I(d)$	0.004 451 7 (5)	0.000 000 39 (0)	8.892 07 (102)	0.000 057 (1)	0.001 225 (8)
$I(e)$	0.010 296 (4)	0.000 001 60 (0)	-1.219 20 (71)	0.000 232 (1)	0.002 372 (2)
$I(f)$	0.008 445 9 (14)	0.000 047 54 (7)	3.685 10 (13)	0.001 231 (6)	0.019 730 (13)
$I(g)^*$	0.028 569 (6)	0.000 023 49 (2)	2.607 87 (38)	0.001 697 (3)	0.002 721 (5)
$I(h)^*$	0.001 696 (13)	-0.000 010 56 (14)	-0.568 61 (104)	0.000 160 (5)	0.001 978 (18)
$I(i)^*$	0.017 47 (11)	0.000 001 67 (3)	0.087 6 (65)	0.000 237 (2)	absent
$I(j)$	0.000 397 5 (18)	0.000 002 3 (1)	-1.263 72 (14)	0.000 149 (2)	0.000 110 (5)

* Generated automatically by *gencodeN* and *gencodevpN*.

Columns 2, 3, 4, 5, 6 list mass-independent terms of a_e , terms of a_e dependent on m_e/m_μ , electron loop contributions to a_μ , tau-lepton loop contribution to a_μ , and terms of a_μ dependent on both m_μ/m_e and m_μ/m_τ , respectively.

Table: Numerical values of diagrams of Sets II, III, and IV. Preliminary results are indicated by **red**.

Set	$A_1^{(10)}$	$A_2^{(10)}(m_e/m_\mu)$	$A_2^{(10)}(m_\mu/m_e)$	$A_2^{(10)}(m_\mu/m_\tau)$	$A_3^{(10)}(m_\mu/m_e, m_\mu/m_\tau)$
III(a)	0.004 13 (9)	-0.000 513 (8)	-70.471 7 (38)	-0.086 88 (74)	-0.523 9 (22)
III(b)	-0.054 22 (4)	-0.000 630 (7)	-34.771 5 (26)	0.004 71 (15)	0.035 90 (94)
III(c)*	-0.116 39 (13)	-0.000 366 (1)	-3.999 5 (72)	-0.125 110 (78)	-0.051 85 (32)
III(d)*	-0.243 00 (29)	-0.000 097 (1)	0.513 7 (85)	-0.007 69 (4)	absent
III(e)*	-1.344 9 (10)	-0.000 465 (4)	3.265 (12)	-0.038 1 (2)	absent
III(f)	-2.434 6 (16)	-0.005 94 (49)	-77.465 (12)	-0.267 5 (65)	-0.505 (27)
III(a)*	2.127 48 (22)	-0.013 69 (11)	109.022 7 (32)	1.021 07 (48)	absent
III(b)*	3.326 94 (33)	0.002 730 (35)	11.936 7 (46)	0.142 6 (12)	absent
III(c)	4.906 (22)	0.003 49 (91)	7.20 (24)	0.202 5 (37)	absent
IV*	-7.736 0 (52)	-0.009 77 (16)	-38.81 (17)	-0.441 3 (40)	absent

* Generated automatically by *gencodeN* and *gencodevpN*.

Columns 2, 3, 4, 5, 6 list mass-independent terms of a_e , terms of a_e dependent on m_e/m_μ , electron loop contributions to a_μ , tau-lepton loop contribution to a_μ , and terms of a_μ dependent on both m_μ/m_e and m_μ/m_τ , respectively.

Set VI containing light-by-light-scattering loop(s) are more difficult.

Table: Numerical values of diagrams of Set VI. Preliminary results are indicated by red.

Set	$A_1^{(10)}$	$A_2^{(10)}(m_e/m_\mu)$	$A_2^{(10)}(m_\mu/m_e)$	$A_2^{(10)}(m_\mu/m_\tau)$	$A_3^{(10)}(m_\mu/m_e, m_\mu/m_\tau)$
VI(a)	1.041 7 (4)	0.004 97 (29)	629.141 (12)	0.227 3 (48)	1.991 (71)
VI(b)	1.347 3 (3)	0.001 742 (47)	181.128 5 (51)	0.095 3 (11)	0.189 3 (32)
VI(c)	-2.592 2 (34)	-0.005 34 (47)	-36.576 (114)	-0.279 3 (77)	-0.478 7 (954)
VI(d)*	1.846 7 (70)	0.001 276 (76)	-7.983 (811)	0.081 77 (151)	absent
VI(e)	-0.431 2 (6)	-0.000 765 (40)	-4.322 (135)	-0.035 77 (57)	-0.118 2 (58)
VI(f)	0.770 3 (24)	-0.000 26 (26)	-38.16 (15)	0.119 (57)	0.173 (11)
VI(g)*	-1.590 4 (63)	-0.000 497 (29)	7.346 (489)	-0.044 51 (96)	absent
VI(h)*	0.179 2 (39)	0.000 045 (10)	-8.546 (231)	0.004 85 (46)	absent
VI(i)	-0.043 8 (11)	-0.000 508 (123)	-27.337 (115)	-0.004 53 (172)	-0.004 1 (77)
VI(j)	-0.228 8 (17)	-0.000 37 (35)	-25.505 (20)	-0.014 2 (63)	0.237 (14)
VI(k)	0.680 2 (38)	0.000 202 (24)	97.123 (62)	0.001 4 (17)	absent

* Generated automatically by *gencodeLLN*.

Columns 2, 3, 4, 5, 6 list mass-independent terms of a_e , terms of a_e dependent on m_e/m_μ , electron loop contributions to a_μ , tau-lepton loop contribution to a_μ , and terms of a_μ dependent on both m_μ/m_e and m_μ/m_τ , respectively.

- Largest and most difficult is Set V, which consists of **6354** Feynman diagrams, more than half of total: **12672**.
- Luckily, Set V has nice feature that the sum $\Lambda^\nu(p, q)$ of 9 vertex diagrams, obtained by inserting an external vertex in the electron lines of a self-energy diagram $\Sigma(p)$, can be expressed in the form

$$\Lambda^\nu(p, q) \simeq -q_\mu \left[\frac{\partial \Lambda_\mu(p, q)}{\partial q_\nu} \right]_{q=0} - \frac{\partial \Sigma(p)}{\partial p_\nu}$$

which is derived from the Ward-Takahashi identity.

- This enables us to cut no. of independent integrals to 706.
- Time-reversal symmetry reduces it to 389. They are shown in next page.

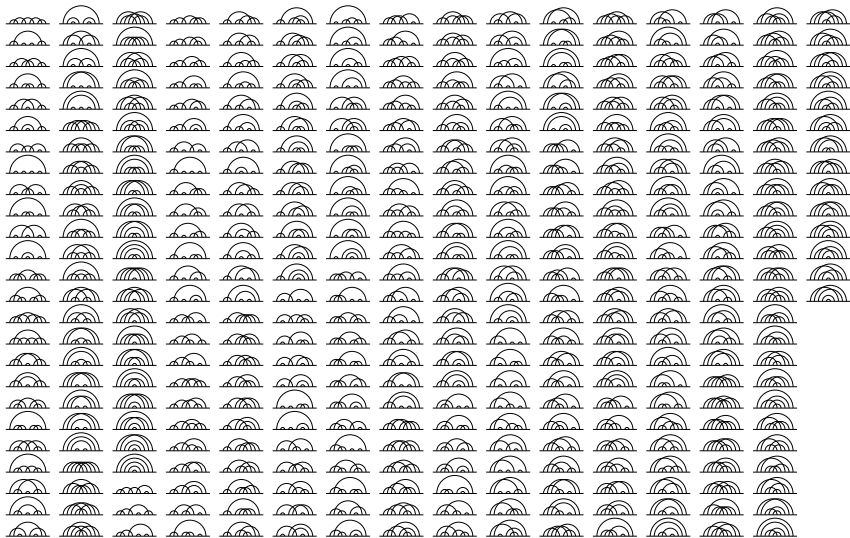
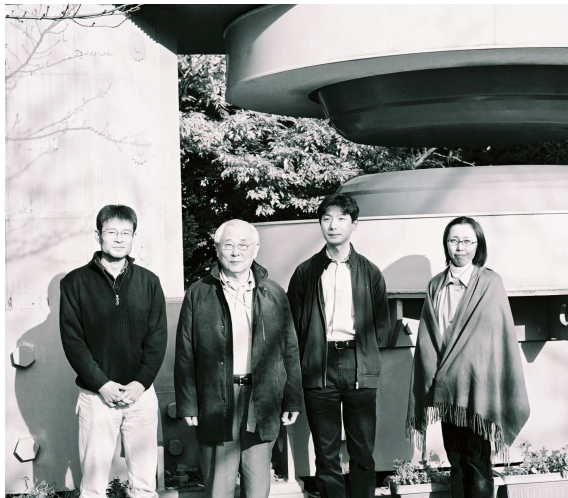


Figure: 389 self-energy diagrams representing 6354 vertex diagrams of Set V.

- It is to handle these diagrams that we developed the automatic code generator *gencodeN*.

T. Aoyama, M. Hayakawa, T. Kinoshita and M. Nio,
Nucl. Phys. B **740**, 138 (2006); B **796**, 184 (2008).



gencodeN consists of several steps:

Step I: Diagram identification

- Specify diagram by vertex pairs connected by virtual photons. This information is stored as plain-text file Xabc (abc = 001, 002, ..., 389).
- Xabc defines not only the diagram itself but also identifies **all UV- and IR-divergent subdiagrams**.
- Implemented by Perl (and C++).

Step II: Construction of unrenormalized integrand

- Translate "Xabc" into mom. integral by Feynman-Dyson rule (by Perl). Output serves as input for [Home-made analytic integration table](#) written in FORM which turns it into a Feynman-parametric integral of the form

$$\int (dz) f(z), \quad (dz) \equiv \prod_{i=1}^N dz_i \delta\left(1 - \sum_{i=1}^N z_i\right).$$

- $f(z)$ is very complicated func. of z and seems nearly intractable.
- However, in terms of "building blocks" B_{ij} , A_i , U , V , it exhibits well-organized structure

$$f(z) = \frac{F_0(B_{ij}, A_i)}{U^2 V^{n-1}} + \frac{F_1(B_{ij}, A_i)}{U^3 V^{n-2}} + \dots$$

Step III: Construction of building blocks

- Express B_{ij} , U , V as polynomials of z_1, z_2, \dots, z_N .
- U , B_{ij} are determined by network topology of loop momenta.
- They are obtained automatically by MAPLE and FORM:

$$X_{abc} \rightarrow B_{ij}, U, \dots$$

- A_i is fraction of external momentum in line i , and satisfies Kirchhoff's loop law and junction law for "currents".
- Form of V is common to all diagrams of Set V:

$$V = \sum_i^{\text{electrons}} z_i (1 - A_i) m^2,$$

where m is lepton mass.

Step IV: Removal of UV divergence

- Renormalization must be performed **exactly to 8th order**.
- Our approach is subtractive renormalization.
- UV divergence arises from subdiagram S identified by $U \rightarrow 0$ for $\Sigma_S Z_i \rightarrow 0$.
- UV-subtraction term is built from original integrand by procedure, called ***K-operation***, which gives UV limits of B_{ij} , A_i , U , V based on a simple power-counting rule.
- Properties of terms generated by *K-operation*:
 - Pointwise subtraction of UV divergence.
 - Subtraction term factorizes analytically into product of lower-order quantities, a feature useful for cross-checking of different diagrams.
 - Gives only UV-divergent parts δm_n^{UV} , L_n^{UV} , B_n^{UV} of renorm. consts. δm_n , L_n , B_n .

Step V: Removal of IR divergence

- These integrals still suffer from IR divergence, logarithmic or worse.
- IR div. is characterized by $V \rightarrow 0$ in subdomain of integration.
- Linear (or worse) IR div., which is caused by the UV-finite term $\widetilde{\delta m}_N \equiv \delta m_N - \delta m_N^{UV}$ ($N > 2$), is difficult to handle directly.
- This problem can be avoided by subtracting $\widetilde{\delta m}_N$ together with the UV-divergent δm_N^{UV} so that full mass renormalization is achieved in Step IV.

T. Aoyama, M. Hayakawa, T. Kinoshita and M. Nio,
Nucl. Phys. B **796**, 184 (2008).

- Remaining logarithmic IR divergence can be handled easily by *l-operation* defined by the IR power counting.

Example: Diagram X072

- An example: Diagram X072.
- Step I produces a file that contains just one-line statement

abcdeedcba

which shows how photons a, b, c, d, e are attached to the electron line.

- This information is sufficient to generate complete instruction for Steps II and III for building 'unrenormalized' integral 'MX072' and also Steps IV and V for building UV-divergent and IR-divergent subintegrals.
- In our renormalization scheme all terms (represented symbolically in next page) are combined to form UV- and IR-finite piece "DMX072".

A shell script controls flow of all Steps automatically:

- (a) Get input information from data "Xabc" prepared in Step I.
 - (b) Build FORTRAN codes following Steps II, III, IV, V.
 - (c) Assemble FORTRAN codes, ready them for numerical integration.
- Numerical integration is carried out by adaptive-iterative Monte-Carlo routine VEGAS.

Lepage, J. Comput. Phys. 27, 192 (1978)

- Snapshot (11/02/2010) of calculation is shown in next pages in 12 columns, 4 columns for each diagram.
- Second column lists number of subtraction terms.
- Fourth column gives CPU time in minutes for $10^7 \times 50$ with 32 cores, in real*8, for mutual comparison. Many results listed are obtained with much higher statistics.

Table: Set V diagrams from X001 - X099

dgrm	sub.	Value (Error)	time	dgrm	sub.	Value (Error)	time	dgrm	sub.	Value (Error)	time
X 1	47	-0.2981(0.0327)	231	X 2	47	-5.9781(0.0462)	177	X 3	19	-0.1142(0.0094)	187
X 4	71	5.1280(0.0541)	241	X 5	43	1.1401(0.0377)	193	X 6	59	-5.2927(0.0433)	166
X 7	47	-3.4833(0.0467)	188	X 8	47	-16.5212(0.0554)	110	X 9	19	-2.8715(0.0584)	161
X 10	83	11.2762(0.0484)	105	X 11	43	6.0549(0.0453)	235	X 12	67	-9.3202(0.0304)	112
X 13	7	-1.3540(0.0038)	160	X 14	31	0.7833(0.0141)	228	X 15	2	2.1020(0.0019)	151
X 16	2	-0.9609(0.0019)	149	X 17	6	0.5174(0.0062)	150	X 18	6	0.0579(0.0069)	145
X 19	31	1.2183(0.0140)	192	X 20	134	-8.1361(0.0564)	90	X 21	11	-0.2967(0.0049)	162
X 22	79	0.9382(0.0433)	117	X 23	27	6.0447(0.0418)	220	X 24	75	-6.1010(0.0426)	119
X 25	39	-0.7824(0.0411)	188	X 26	95	-7.8186(0.0336)	98	X 27	15	-2.3190(0.0315)	166
X 28	71	4.5631(0.0588)	119	X 29	35	6.8839(0.0333)	167	X 30	67	-12.6108(0.0386)	99
X 31	2	2.2932(0.0029)	143	X 32	2	-0.2427(0.0013)	139	X 33	2	-1.3771(0.0014)	131
X 34	2	1.2539(0.0021)	140	X 35	2	-0.5838(0.0014)	145	X 36	11	0.2473(0.0064)	68
X 37	2	-0.7417(0.0020)	148	X 38	11	-0.2811(0.0049)	65	X 39	11	0.3164(0.0044)	208
X 40	47	1.4835(0.0314)	87	X 41	63	3.1418(0.0577)	175	X 42	119	-4.1234(0.0418)	84
X 43	15	-2.8829(0.0356)	149	X 44	59	4.4462(0.0399)	105	X 45	43	3.4311(0.0324)	118
X 46	95	-7.7361(0.0446)	88	X 47	2	-4.4551(0.0033)	125	X 48	2	-0.8051(0.0016)	135
X 49	2	-0.0295(0.0013)	130	X 50	2	-1.2222(0.0018)	123	X 51	2	-0.1733(0.0020)	148
X 52	11	0.9875(0.0094)	68	X 53	2	0.3646(0.0015)	144	X 54	11	-0.4924(0.0070)	65
X 55	2	-0.3634(0.0014)	146	X 56	11	-0.2408(0.0054)	68	X 57	23	2.6504(0.0164)	113
X 58	44	-5.1538(0.0331)	57	X 59	23	2.1860(0.0176)	142	X 60	92	-3.2758(0.0480)	90
X 61	68	-3.7959(0.0325)	100	X 62	161	5.9124(0.0428)	83	X 63	6	3.3563(0.0086)	143
X 64	6	-0.2763(0.0069)	145	X 65	6	0.1748(0.0055)	156	X 66	26	-3.5299(0.0396)	87
X 67	50	-1.7091(0.0660)	130	X 68	98	2.7344(0.0491)	86	X 69	18	-1.1586(0.0260)	110
X 70	70	3.2263(0.0329)	88	X 71	54	3.6918(0.0215)	100	X 72	134	-5.5392(0.0455)	86
X 73	47	3.4045(0.0448)	190	X 74	47	4.3918(0.0477)	199	X 75	47	-8.1355(0.0496)	165
X 76	19	-5.2424(0.0230)	176	X 77	39	3.2616(0.0443)	226	X 78	39	0.9403(0.0453)	225
X 79	71	5.4206(0.0466)	205	X 80	43	0.5166(0.0502)	206	X 81	59	-5.6569(0.0470)	152
X 82	47	-8.5074(0.0637)	202	X 83	47	18.7382(0.0475)	161	X 84	19	8.9855(0.0278)	173
X 85	39	-2.2692(0.0447)	217	X 86	39	0.5038(0.0442)	182	X 87	77	-16.5708(0.0650)	134
X 88	43	-5.2642(0.0480)	204	X 89	63	12.6876(0.0446)	138	X 90	19	1.5108(0.0294)	160
X 91	39	-1.8168(0.0486)	235	X 92	39	2.1022(0.0454)	194	X 93	7	-1.7604(0.0050)	160
X 94	15	-1.0460(0.0099)	194	X 95	7	0.5791(0.0043)	159	X 96	31	1.2849(0.0179)	196
X 97	17	4.7894(0.0593)	168	X 98	33	-1.9365(0.0370)	169	X 99	39	3.0813(0.0434)	195

Table: Set V diagrams from X100 - X198

dgrm	sub.	Value (Error)	time	dgrm	sub.	Value (Error)	time	dgrm	sub.	Value (Error)	time
X100	77	-15.3143(0.0627)	136	X101	15	-0.2625(0.0093)	188	X102	31	-1.3912(0.0312)	235
X103	31	0.8229(0.0193)	216	X104	79	6.4712(0.0581)	165	X105	35	3.0633(0.0487)	191
X106	71	-11.5433(0.0492)	136	X107	43	-4.6615(0.0584)	200	X108	63	12.9649(0.0440)	142
X109	17	0.0220(0.0440)	166	X110	35	1.9409(0.0417)	183	X111	33	3.4365(0.0688)	175
X112	71	-11.8915(0.0481)	136	X113	39	-4.4510(0.0545)	162	X114	63	11.0810(0.0468)	122
X115	7	-0.5947(0.0065)	158	X116	7	1.8059(0.0050)	161	X117	7	0.3232(0.0045)	157
X118	15	-3.2225(0.0106)	171	X119	15	-0.1055(0.0113)	197	X120	31	1.7913(0.0158)	194
X121	7	-0.8630(0.0044)	167	X122	7	-0.7414(0.0042)	162	X123	15	-3.3339(0.0075)	176
X124	29	11.1936(0.0631)	107	X125	31	0.7481(0.0189)	221	X126	59	-1.2410(0.0625)	139
X127	15	1.1349(0.0059)	192	X128	31	0.5916(0.0129)	198	X129	31	1.4312(0.0123)	220
X130	59	-1.5371(0.0393)	138	X131	59	3.1603(0.0727)	191	X132	101	-8.8220(0.0588)	125
X133	17	2.6477(0.0423)	172	X134	33	-0.4814(0.0641)	170	X135	33	1.0868(0.0659)	180
X136	65	-7.5387(0.0569)	137	X137	45	-2.5009(0.0739)	131	X138	85	10.1410(0.0480)	105
X139	47	14.8592(0.0502)	205	X140	39	-2.7411(0.0465)	156	X141	74	-12.5628(0.0680)	165
X142	43	-1.6913(0.0700)	189	X143	61	10.3414(0.0433)	154	X144	83	23.7308(0.0662)	103
X145	67	-18.6357(0.0471)	111	X146	39	-2.3801(0.0690)	200	X147	15	1.1276(0.0223)	149
X148	31	-1.3144(0.0364)	168	X149	17	-8.3912(0.0309)	164	X150	33	2.8037(0.0614)	195
X151	87	-10.8607(0.0603)	94	X152	77	14.6570(0.0480)	107	X153	77	14.9037(0.0559)	106
X154	67	-20.5911(0.0539)	102	X155	15	4.9510(0.0225)	169	X156	31	-0.7363(0.0454)	172
X157	32	-11.8522(0.0408)	69	X158	65	0.4466(0.0539)	83	X159	65	0.2208(0.0733)	84
X160	116	14.0278(0.0599)	96	X161	71	7.7606(0.0428)	102	X162	95	-12.8160(0.0408)	95
X163	19	6.6451(0.0702)	173	X164	19	-12.0134(0.0639)	137	X165	15	-2.1380(0.0114)	181
X166	15	-2.2856(0.0121)	169	X167	29	12.1602(0.0338)	115	X168	17	3.3651(0.0573)	158
X169	25	-6.9274(0.0247)	106	X170	39	0.2847(0.0573)	178	X171	39	-2.6059(0.0529)	164
X172	31	1.4301(0.0225)	214	X173	59	0.2731(0.0737)	237	X174	35	1.8660(0.0602)	177
X175	51	-1.8412(0.0397)	151	X176	7	0.7651(0.0184)	153	X177	15	-0.0111(0.0352)	149
X178	5	0.7079(0.0038)	153	X179	2	-0.4378(0.0034)	142	X180	11	0.0242(0.0044)	147
X181	6	-4.3571(0.0146)	142	X182	12	1.2875(0.0157)	167	X183	7	-0.0179(0.0186)	140
X184	31	0.4381(0.0637)	170	X185	5	-0.1313(0.0050)	142	X186	23	1.1634(0.0049)	195
X187	6	1.2832(0.0128)	137	X188	24	1.8185(0.0232)	190	X189	17	-3.7335(0.0226)	162
X190	33	-2.4993(0.0359)	193	X191	13	0.1938(0.0246)	150	X192	25	2.4665(0.0438)	175
X193	15	-4.2494(0.0175)	139	X194	27	-0.8543(0.0652)	163	X195	2	-1.0665(0.0045)	158
X196	2	-2.0375(0.0029)	130	X197	2	-0.3870(0.0022)	148	X198	5	-2.3452(0.0027)	132

Table: Set V diagrams from X199 - X297

dgrm	sub.	Value (Error)	time	dgrm	sub.	Value (Error)	time	dgrm	sub.	Value (Error)	time
X199	5	1.0493(0.0038)	145	X200	11	0.0092(0.0043)	151	X201	2	-0.4877(0.0037)	140
X202	2	1.9243(0.0030)	128	X203	2	0.9037(0.0023)	147	X204	11	-1.9324(0.0038)	158
X205	5	-0.9038(0.0049)	152	X206	23	1.6447(0.0065)	191	X207	5	0.2894(0.0042)	163
X208	11	0.5215(0.0040)	154	X209	5	0.1444(0.0040)	160	X210	23	0.7653(0.0049)	190
X211	23	5.1027(0.0348)	119	X212	41	-0.3297(0.0554)	173	X213	6	-2.4132(0.0118)	145
X214	12	0.6646(0.0142)	140	X215	6	0.1151(0.0120)	145	X216	24	-1.1993(0.0239)	164
X217	18	-2.2056(0.0537)	106	X218	30	-1.7370(0.0670)	130	X219	39	1.3630(0.0488)	173
X220	59	-2.4828(0.0511)	210	X221	35	0.6897(0.0347)	167	X222	51	0.8242(0.0386)	143
X223	116	17.4832(0.0543)	100	X224	31	2.4650(0.0232)	202	X225	23	0.2928(0.0098)	216
X226	13	1.0518(0.0231)	153	X227	25	0.6828(0.0398)	181	X228	75	-6.7788(0.0664)	108
X229	35	-1.9956(0.0651)	204	X230	71	15.6775(0.0549)	109	X231	11	-0.7467(0.0058)	177
X232	23	0.4010(0.0116)	215	X233	31	8.5433(0.0434)	79	X234	63	-2.4968(0.0460)	97
X235	23	0.7040(0.0100)	245	X236	63	2.0658(0.0381)	112	X237	113	-13.0105(0.0645)	104
X238	25	1.4003(0.0391)	180	X239	69	-2.8983(0.0645)	108	X240	93	10.9598(0.0571)	96
X241	43	13.8540(0.0634)	210	X242	68	-10.5143(0.0659)	195	X243	57	3.8884(0.0582)	176
X244	35	-3.3003(0.0654)	200	X245	27	0.0824(0.0338)	176	X246	29	-0.4379(0.0365)	192
X247	39	15.9448(0.0552)	213	X248	31	-1.9496(0.0459)	161	X249	13	3.9940(0.0159)	156
X250	27	-0.8949(0.0402)	172	X251	27	-1.2982(0.0300)	170	X252	56	-10.9812(0.0691)	141
X253	113	17.8089(0.0672)	86	X254	29	2.1746(0.0392)	192	X255	43	8.1509(0.0541)	140
X256	93	-14.0506(0.0543)	93	X257	7	5.6299(0.0259)	133	X258	7	-0.4470(0.0168)	155
X259	5	0.0160(0.0049)	141	X260	5	-0.4007(0.0036)	165	X261	6	6.3373(0.0172)	132
X262	6	-2.2800(0.0140)	153	X263	7	-2.7605(0.0144)	142	X264	15	4.7945(0.0346)	156
X265	5	-0.6741(0.0034)	141	X266	11	0.1179(0.0048)	167	X267	6	-0.6336(0.0099)	138
X268	12	0.1262(0.0191)	156	X269	15	-0.6542(0.0308)	171	X270	31	-1.5919(0.0607)	173
X271	11	0.2415(0.0053)	205	X272	23	-0.7339(0.0093)	217	X273	13	-2.0001(0.0240)	165
X274	25	0.8899(0.0406)	175	X275	2	-0.7434(0.0044)	126	X276	2	-0.5544(0.0028)	133
X277	2	2.7843(0.0015)	185	X278	5	-0.1559(0.0044)	144	X279	5	0.8231(0.0038)	164
X280	2	-1.0096(0.0046)	130	X281	5	-1.3724(0.0041)	154	X282	5	0.4841(0.0034)	148
X283	11	-0.0505(0.0042)	167	X284	2	-0.2711(0.0032)	159	X285	5	0.0169(0.0039)	152
X286	11	0.7775(0.0038)	186	X287	23	0.1874(0.0068)	190	X288	6	4.1604(0.0152)	130
X289	6	-1.5135(0.0130)	152	X290	6	-3.7248(0.0117)	143	X291	12	1.5878(0.0178)	158
X292	12	0.9126(0.0149)	163	X293	24	-1.1657(0.0266)	167	X294	7	-3.3322(0.0166)	150
X295	7	1.7876(0.0186)	151	X296	5	0.5448(0.0046)	170	X297	5	-0.4792(0.0047)	160

Table: Set V diagrams from X298 - X389

dgrm	sub.	Value (Error)	time	dgrm	sub.	Value (Error)	time	dgrm	sub.	Value (Error)	time
X298	6	-1.8909(0.0115)	158	X299	6	-0.2647(0.0122)	155	X300	29	-9.3516(0.0580)	84
X301	31	-1.0812(0.0672)	184	X302	59	-1.8824(0.0523)	105	X303	2	0.3213(0.0025)	152
X304	5	-0.3422(0.0049)	165	X305	5	0.4619(0.0040)	167	X306	23	0.1582(0.0226)	71
X307	47	-0.1151(0.0397)	88	X308	6	1.8367(0.0145)	154	X309	26	-4.2650(0.0376)	84
X310	50	-0.0629(0.0737)	100	X311	15	-0.4378(0.0278)	165	X312	31	-1.1090(0.0534)	177
X313	11	0.9513(0.0043)	192	X314	23	0.7992(0.0070)	203	X315	13	-1.2886(0.0216)	163
X316	25	0.1050(0.0338)	187	X317	59	1.3935(0.0522)	106	X318	62	-8.7913(0.0674)	170
X319	47	0.7468(0.0678)	204	X320	11	0.5585(0.0045)	168	X321	23	-0.9154(0.0078)	237
X322	23	0.9205(0.0032)	189	X323	25	0.0954(0.0331)	173	X324	53	-8.8189(0.0510)	133
X325	107	11.6018(0.0571)	93	X326	17	-8.8868(0.0557)	170	X327	33	1.4993(0.0617)	192
X328	13	-0.2799(0.0191)	163	X329	25	-0.8929(0.0252)	180	X330	15	-4.8847(0.0546)	174
X331	27	4.4591(0.0628)	194	X332	33	2.8378(0.0722)	195	X333	65	6.7152(0.0634)	122
X334	47	5.2084(0.0554)	163	X335	37	-2.0700(0.0568)	139	X336	6	-0.7509(0.0076)	153
X337	12	-1.1895(0.0143)	146	X338	13	-1.8395(0.0208)	168	X339	25	0.4930(0.0283)	169
X340	53	-2.2777(0.0676)	93	X341	24	1.8004(0.0137)	156	X342	27	2.5993(0.0173)	157
X343	2	3.8805(0.0029)	149	X344	2	3.4147(0.0037)	122	X345	2	-1.0015(0.0024)	153
X346	2	0.2844(0.0037)	138	X347	2	-2.6792(0.0028)	149	X348	2	-0.4859(0.0038)	149
X349	5	2.0816(0.0043)	151	X350	2	1.4548(0.0023)	143	X351	5	0.2449(0.0034)	155
X352	2	-0.1319(0.0025)	157	X353	5	0.1884(0.0025)	169	X354	5	-2.0375(0.0025)	148
X355	11	-1.0637(0.0031)	162	X356	5	2.0708(0.0049)	161	X357	5	0.3634(0.0037)	168
X358	5	0.0333(0.0043)	165	X359	11	-0.1515(0.0046)	170	X360	11	-0.4709(0.0042)	182
X361	23	2.5319(0.0064)	201	X362	2	-0.5660(0.0036)	147	X363	2	-2.3416(0.0022)	141
X364	2	2.3899(0.0021)	147	X365	11	0.4884(0.0115)	62	X366	23	5.6077(0.0222)	65
X367	5	-0.7180(0.0049)	171	X368	23	-0.2878(0.0180)	68	X369	47	-3.2062(0.0395)	77
X370	5	-1.4791(0.0045)	155	X371	5	-0.0074(0.0042)	154	X372	11	-1.2875(0.0025)	162
X373	23	0.5684(0.0039)	183	X374	47	0.9446(0.0533)	147	X375	89	0.8509(0.0589)	68
X376	5	1.0369(0.0034)	164	X377	11	0.4192(0.0036)	188	X378	11	1.3081(0.0034)	176
X379	23	-0.3402(0.0052)	198	X380	47	-0.9354(0.0359)	76	X381	23	1.0677(0.0038)	187
X382	41	-1.6457(0.0389)	183	X383	6	-4.7039(0.0136)	151	X384	12	1.9230(0.0184)	158
X385	12	-0.6982(0.0141)	157	X386	24	0.7383(0.0244)	163	X387	50	1.7962(0.0748)	89
X388	24	-0.3893(0.0199)	163	X389	30	-0.2604(0.0589)	127				

Statistics of running Set V:

- 10–20 minutes for generating FORTRAN code for each diagram on HP Alpha.
- Typical integrand consists of 90,000 lines of FORTRAN code occupying more than 6 Megabytes.
- Evaluation of integral in real*8 with 10^7 sampling points \times 50 iterations takes 2 – 4 hours on 32 cores of RICC (RIKEN Integrated Clusters of Clusters).
- Evaluation in real*16 is about 10 times slower.
- Large runs: real*16, $10^9 \times 100$, takes about 24 days on 256 cores of RICC.

VI: Residual renormalization

- Integrals in these Tables are UV- and IR-finite, but not standard renormalized amplitudes.
- Thus finite adjustment, called **residual renormalization**, must be carried out to get observable $g-2$.
- **Residual renormalization** of all diagrams of Set V requires systematic handling of more than 10,000 integrals.

- Fortunately, they can be organized into 16 terms whose structures are readily recognizable in terms of lower-order quantities

$$\begin{aligned}
a_{10} = & \Delta M_{10} \\
& + \Delta M_8 \left(-7\Delta LB_2 \right) \\
& + \Delta M_6 \left(-5\Delta LB_4 + 20(\Delta LB_2)^2 \right) \\
& + \Delta M_4 \left(-3\Delta LB_6 + 24\Delta LB_2\Delta LB_4 - 28(\Delta LB_2)^3 + 2\Delta L_{2*}\Delta\delta m_4 \right) \\
& + \Delta M_2 \left(-\Delta LB_8 + 4(\Delta LB_4)^2 + 8\Delta LB_2\Delta LB_6 - 28(\Delta LB_2)^2\Delta LB_4 + 14(\Delta LB_2)^4 \right. \\
& \quad \left. + 2\Delta L_{2*}\Delta\delta m_6 - 2\Delta L_{2*}\Delta\delta m_{2*}\Delta\delta m_4 - 16\Delta L_{2*}\Delta LB_2\Delta\delta m_4 + \Delta L_{4*}\Delta\delta m_4 \right)
\end{aligned}$$

where ΔM_n is the finite part of the n -th order magnetic moment,
 ΔLB_n is the sum of finite parts of the n -th order vertex renormalization constant ΔL_n and the wavefunction renormalization constant ΔB_n ,
 $\Delta\delta m_n$ is the finite part of the n -th order selfmass of the electron,
 ΔL_{n*} is obtained from ΔL_n by insertion of 2-vertex in the electron line.

- When residual renormalization is included entire FORTRAN codes becomes analytically exact. No approximation involved.
- Uncertainty of numerical value arises only from numerical integration, which is performed by adaptive-iterative Monte-Carlo routine VEGAS.

- Latest value (11/02/2010) of the sum of 389 integrals and residual renormalization terms is

$$A_1^{(10)}[\text{Set V}] = 9.752 (733) \text{ [Preliminary]}$$

- Uncertainty is being reduced further.
- To obtain $A_1^{(10)}[\text{all}]$ we must add values of other 31 sets. This leads to

$$A_1^{(10)}[\text{all}] = 4.364 (733) \text{ [Preliminary]}$$

- This is still very crude but is already about 6 times more precise than the previous gestimate $|A_1^{(10)}| < 4.6$.

- We are also working to reduce the uncertainty of $A_1^{(8)}$.
- The latest value (11/02/2010) is

$$A_1^{(8)} = -1.910\ 8\ (25) \quad [\textit{Preliminary}]$$

- In terms of these values of $A_1^{(8)}$ and $A_1^{(10)}$ we find

$$\alpha^{-1}(a_e) = 137.035\ 999\ 132\ (9)(6)(33) \\ [0.254\ \textit{ppb}], \quad [\textit{Preliminary}]$$

where 9, 6, 33 are uncertainties of 8th-order, 10th-order, and $a_e(\text{exp})$.

- This is **about 30 times more precise than $\alpha^{-1}(Rb)$** .
- Further progress now depends on improving $a_e(\text{exp})$.

- Discoverers of QED regarded the renormalization procedure as a **jelly-built** temporary fix to be replaced by something better.

Tomonaga: Private communication.

Letter of Dyson to Gabrielse quoted in Physics Today (August 2006), p.15.

From Freeman Dyson – One Inventor of QED ^{Gabrielse}

Dear Jerry,

... I love your way of doing experiments, and I am happy to congratulate you for this latest triumph. Thank you for sending the two papers.

Your statement, that QED is tested far more stringently than its inventors could ever have envisioned, is correct. As one of the inventors, I remember that we thought of QED in 1949 as a temporary and jerry-built structure, with mathematical inconsistencies and renormalized infinities swept under the rug. We did not expect it to last more than ten years before some more solidly built theory would replace it. We expected and hoped that some new experiments would reveal discrepancies that would point the way to a better theory. And now, 57 years have gone by and that ramshackle structure still stands. The theorists ... have kept pace with your experiments, pushing their calculations to higher accuracy than we ever imagined. And you still did not find the discrepancy that we hoped for. To me it remains perpetually amazing that Nature dances to the tune that we scribbled so carelessly 57 years ago. And it is amazing that you can measure her dance to one part per trillion and find her still following our beat.

With congratulations and good wishes for more such beautiful experiments, yours ever, Freeman.

- In fact it was soon found that QED must be enlarged to include hadronic and weak interactions, which led to the Standard Model (SM).
- But **jelly-built** structure itself remained as the basic framework of SM.
- SM itself is generally regarded as temporary measure which requires further modification to accommodate new physics.
- Such modification is most likely to come from experiments at high energy accelerators such as LHC.
- However, impact of new physics on a_e may not necessarily be straightforward.

- As a matter of fact, it might have no detectable effect on $g-2$.
- Reason: Independent α 's measured by non-QED means must also include the effect of new physics.
- Recall that masses and charges involved in ordinary QM cannot be correctly identified as physical mass and charge to the precision that requires radiative corrections.
- For proper interpretation the ordinary QM, by which these measurements of α are interpreted, must be extended to include these effects.
- Such a formulation was obtained for one- and two-body systems as the nonrelativistic limit of explicitly renormalized QED (or SM), unfortunately misnamed NRQED.

Caswell, Lepage, PL 167B, 437 (1986)

- As far as I know, no attempt has been made thus far to extend it to many-particle systems.

- To conclude, the **jelly-built** structure still looks good at the precision exceeding 1 part in 10^9 .
- If disagreement is detected at the next level of precision it might indicate that breakdown of SM comes, not necessarily from high energy region, but from an entirely unexpected direction.
- Unfortunately such an event may not be detectable until α is measured by some independent method with precision comparable to that of $\alpha(a_e)$.
- Until then, $\alpha(a_e)$ serves as the yardstick by which validity of other types of measurements and their theories is examined.